Self-assembly and ordering mechanisms of Ge islands on prepatterned Si(001)

A. Pascale,[1] I. Berbezier,[1,*] A. Ronda,[1] and P. C. Kelires[2,3]
[1]*L2MP-CNRS, Université Paul Cézanne, Campus de St. Jérôme, Case 142, Avenue Escadrille Normandie Niemen, F13397 Marseille Cedex 20, France*
[2]*Physics Department, University of Crete, P.O. Box 2208, 710 03 Heraclion, Crete, Greece*
[3]*Department of Mechanical Engineering and Materials Science and Technology, Cyprus University of Technology, P.O. Box 50329, 3036 Limassol, Cyprus*
(Received 26 July 2007; published 11 February 2008)

Ge deposition on Si(001) substrates patterned by focused ion beams is a promising route toward fabricating highly ordered quantum dots. Depending on the growth temperature T, remarkable orderings of the assembled islands are observed. At low T's, when diffusion is limited, a metastable phase with dots nucleating in the holes prevails. At high T's, when diffusion is not limited by kinetics, an equilibrium ordered phase is observed with dots nucleating on the terraces in between the pits. At intermediate T's, random growth arises. Monte Carlo simulations shed light onto this phenomenon. It is shown that the average stress energy of the equilibrium ordered configuration is significantly lower than the energy of configurations with islands positioned in the pits. Random nucleation gives rise to saddle configurations between the two ordered phases.

DOI: 10.1103/PhysRevB.77.075311 PACS number(s): 68.65.Hb, 61.46.Hk, 68.55.A−

Predicting and understanding the self-assembly of heteroepitaxial quantum dots (QDs) are challenging problems. A prototypical example is given by Ge islands grown during Ge/Si heteroepitaxy. Research efforts on the self-assembling properties of these islands are motivated by both fundamental physics and promising applications in nanoelectronics. Not surprisingly, many studies have been devoted to the development of techniques that would be capable of enhancing self-assembly and ordering. However, none of these fabrication techniques have succeeded in perfectly ordering high density of ultrasmall Ge QD on Si substrates (with QD sizes and densities about 10 nm and $10^{11}/\mathrm{cm}^2$, respectively).

The key to the successful creation of ordered island configurations lies in the controlled generation of nanopatterns, which can provide nucleation sites for the dots and at the same time relieve the heteroepitaxial stress. Mechanisms that are spontaneously activated to relieve the stress in the QD and in surroundings regions in nominal surfaces include, depending on the growth temperature T, the nucleation of misfit dislocations, intermixing of species, and trench formation.[1–7] However, these generic mechanisms are not so relevant to the desired QD ordering. On the other hand, the growth of perfectly ordered QD on artificial nanopatterns produced by lithography, such as stripes, mesas, or holes, has been shown to produce a perfect ordering of the dots,[8–14] but not yet at the desired level of size or density for nanoelectronic applications (which need QD sizes of about 10–15 nm and densities larger than $10^{11}/\mathrm{cm}^2$). The driving force behind this preferential nucleation is still under debate.[15–17]

In this paper, we demonstrate that the use of Si(001) substrates prepatterned by the focused ion beam (FIB) technique allows to create well-ordered small and dense arrays of Ge QDs. The main advantage of FIB is the direct writing with ultrahigh resolution which permits the creation of highly dense ($\sim 2.10^{11}/\mathrm{cm}^2$) and ultrasmall patterns (lateral size $\sim$10 nm).[18] We show that at high deposition temperatures T's, when nucleation is not limited by kinetics, Ge islands remarkably order on terraces close or between the pits (holes) produced by FIB. On the other hand, at low T's, nicely ordered configurations with islands in the pits are formed.[18] We explain this remarkable behavior through state-of-the-art Monte Carlo (MC) simulations. We show that for pit patterns consisting of 2 or more monolayer (ML) -height steps, islands prefer to locate on the terraces between the pits rather than on the stepped pit walls because this considerably reduces the average energy and stress in the grown overlayer. This suggests that islands grown at low T's in the pits are metastable structures which are not promoted by energy minimization of the structure.

The experimental analysis is based on Ge islands, which were self-organized on nanopatterned Si substrates using a solid-source molecular beam epitaxy system with a background pressure in the 10^{-11} Torr range. Nominal Si(001) substrates with a resistivity of about 10 Ω/cm have been used. Ge and Si fluxes were obtained from an effusion Knudsen cell and an electron beam evaporator, respectively. The patterning of Si substrates was produced by FIB milling using a gallium liquid metal primary ion gun. The dimensions of the FIB holes varied between 20 and 100 nm laterally and between 2 and 40 nm in height. After FIB milling, Ga was fully removed by a special chemical cleaning procedure.[18] Perfectly clean and reproducible Si(001) surfaces were obtained after *in situ* thermal flash at 900 °C by the deposition of a 4 nm thick Si buffer layer. After total removal of Ga, we checked by atomic force microscopy (AFM) before Ge deposition that the Si buffer layer follows a perfect two-dimensional growth.[19] Ge was deposited at 550, 650, and 750 °C at a growth rate of 0.03 nm/s. The island morphologies and positions were investigated *ex situ* by AFM.

The central question arising, in general, when deposition takes place on a patterned surface is whether the patterns represent preferential sites for island nucleation. In the present case, the FIB method produces a highly uniform and dense array of holes (pits), which are likely to be stepped and which can serve as initial island nucleation sites. Therefore, it is extremely interesting to investigate whether the islands have a clear tendency to nucleate and grow inside the pits,

along the stepped walls, or on the terraces between the pits and how this relates to the growth T's. In either case, such a tendency would give rise to a well-ordered array of islands. If no clear tendency exists, a random distribution of islands both on terraces and in pits would likely to be the preferred configuration.

Our experimental investigations addressed this kind of questions and revealed a remarkable tendency of Ge QD to grow in ordered configurations. However, this depends strongly on the growth T's. At high T's, under conditions of enhanced surface diffusivity, the dots grow orderly on the flat terraces between the pit patterns. This phenomenon is well evidenced by the AFM image of a FIB patterned area after Ge deposition at 750 °C. Figure 1(a) demonstrates the creation of well-ordered island configurations, such as the one where three Ge dots are located exactly between holes [Fig. 1(a) inset]. We can clearly distinguish in the image four pits surrounding each Ge dot. Both due to the high deposition T's and the associated high surface diffusion, which induce large islands, and the limited amount (8 ML) of Ge deposited, which induces a low island density, not a complete filling of the areas between the pits is obtained. By optimizing these parameters, a denser ordered configuration can be readily achieved.

A similar positioning of islands has been observed when pits have smaller dimensions with a lateral size of ~20 nm and depth of ~2 nm (not shown). When the distance between the holes becomes much larger than the island lateral size, the nucleation still takes place on the flat terraces but close to the pit edges [Fig. 1(b)]. Similar Ge island locations were previously observed close to scanning tunneling microscopy (STM) nanopatterns with a smaller pit height.[20] This indicates that there exists an attraction of the islands by the stress field of the nanopatterns.

On the other hand, at a low deposition T of 550 °C, when kinetics is limited and smaller islands are formed, we observe a perfect ordered distribution of islands inside the pits, as it is clearly demonstrated by the AFM image in Fig. 1(d). Interestingly, at intermediate T of 650 °C, a random distribution arises and the nucleation of islands occurs both on terraces and inside the pits [Fig. 1(c)]. This seems to be a transition state between the two ordered configurations. These experimental results suggest that at low deposition T's the stepped pit walls act as nucleation sites and that islands, once nucleated, grow solely inside the pits. On the contrary, at high T's, although the holes might still act as nucleation sites, they are not favorable positions for the dots anymore. It is clear that the ordering of islands critically depends on the deposition temperature and on atomic mobility. Thus, there seems to be interplay between equilibrium and metastability which drives the island self-organization.

In order to explain and gain insight into this remarkable behavior, we carried out continuous-space MC simulations of the equilibrium structure, stress state, and energetics of Ge islands on patterned Si(001) surfaces. The method has been used with success and described extensively in similar studies related to stress and intermixing in Ge QD on nominal Si(001) surfaces.[21,22] The interactions are modeled using the well established interatomic potentials of Tersoff for multicomponent systems.[23] Bonding and strain fields induced by

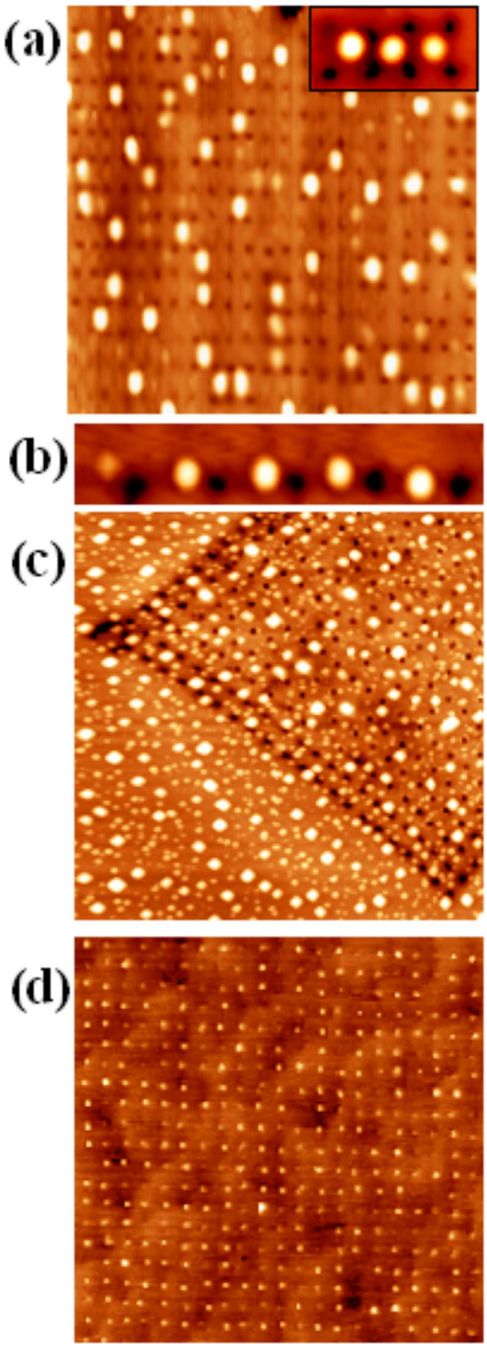

FIG. 1. (Color online) AFM images of FIB patterned areas after 8 ML Ge deposition at different temperatures (T_G): (a) T_G=750 °C. In this situation, the size of QD (100 nm) is in the range of the hole-hole distance (150 nm). The inset shows a higher magnification image of three Ge QDs situated on terraces between the FIB pits. (b) T_G=750 °C. In this situation, the size of QD is three times smaller than the hole-hole distance (350 nm). Ge QDs are located close to FIB pits. The image horizontal size is 1.7 μm. (c) T_G =650 °C; hole-hole distance is 150 nm. In this situation, Ge QDs are located randomly both in the holes and out of the holes. (d) T_G=550 °C. In this situation, Ge QDs are located only in the holes. Scan size is 2.5 μm in (a), (c), and (d).

the Si(001)-2×1 surface reconstruction are accurately described.[24] This implies that the stress fields due to islanding are correctly modeled when the top of the wetting layer

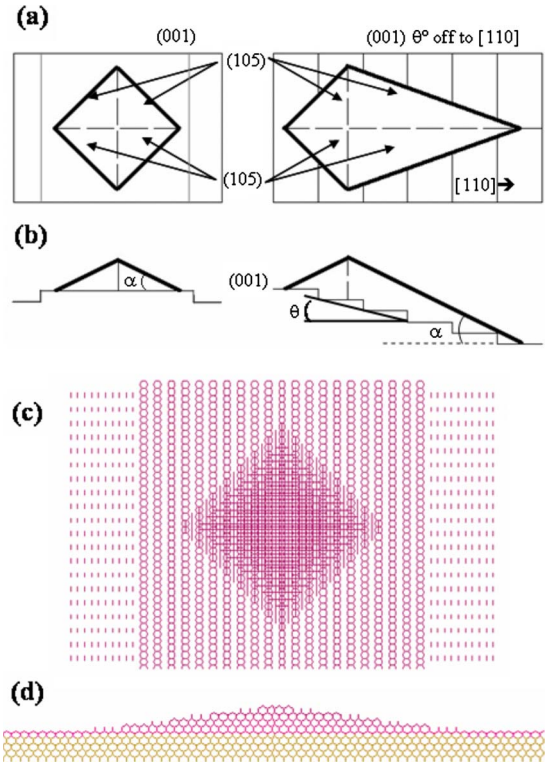

FIG. 2. (Color online) (a) Top view and (b) side view of a pyramidal island with {105} facets located on the terrace between two holes (left) and on the side of the hole (right). (c) Top view and (d) side view of the simulated structure consisting of a Ge island on top of the $2\times1-1\times2$ reconstructed Ge WL (between pits) itself on top of the Si substrate.

(WL) and the island facets have 2×1 reconstruction.

In this empirical scheme, one calculates the cohesive (total) energy E of the system, resulting from Gibb's free-energy minimization at finite T's, and can furthermore decompose it into atomic contributions. This advantageous property gives us the capability to define energy-dependent atomic level quantities. For the purposes of the present work, the key such quantity is the atomic level stress,[25] which locally analyzes the stress field in the structure. It is defined by $\sigma_i=-dE_i/d\ln V\sim p\Omega_i$, where E_i is the energy of atom i and V is the volume. Dividing by the appropriate atomic volume, Ω_i converts into units of pressure p.[24] The σ_i's can be summed up over a specific region to yield the average stress of this region. Since E, and thus E_i, encompasses all possible contributions, including surface energies, the so-defined atomic stresses fully describe all driving factors governing island nucleation and growth.

The simulated structures consist of Ge islands on top of a WL of Ge and a Si substrate in the (001) orientation, in the presence of pit patterns representing the holes produced by the FIB method (Fig. 2). In order to address the problem as accurately as possible, our model specifically takes into account the atomistic environment in the pits. So, the pit walls are modeled as consisting of trains of monolayer height steps. We assume that when islands grow inside the holes, they nucleate along this sequence of steps in agreement with experimental observations evidencing the nucleation of islands at the step edges of the silicon surface.[26] For simplicity and to make the simulations tractable, we only consider pyramidal-shape islands. When the islands are located at the middle of terraces between pits, they have a square base and {105} facets. When they are located on the sequence of steps, they are elongated perpendicular to the step edges in order to preserve the {105} faceting, which is essential for surface energy minimization.[27–29] The relevant geometries are portrayed in Fig. 2. Figures 2(c) and 2(d) show the top view and the side view of a simulated cell (in the situation where the island is located on the terrace, between pit patterns), respectively. The base of the island is oriented at an angle of 45° with respect to the dimer rows of the WL.

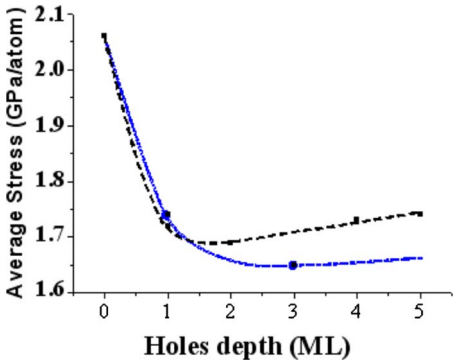

FIG. 3. (Color online) Stress of QD structures on a patterned Si(001) as a function of the hole depth (height is measured in monatomic step scale). Values for structures with islands located on the hole side (terrace) are denoted by a dotted line (solid line).

The top layer of the WL and (105) faceted pyramids are reconstructed in the usual 2×1 dimer configuration [Fig. 2(c)]. We took care that the pit walls consist of alternating S_A and S_B steps (T_A and T_B terraces), with the dimer rows running parallel and perpendicular to the step edges, respectively. The width of the WL is 3 ML, while the Si substrate consists of 8 ML. The bottom layer is kept fixed throughout the simulation. Due to the limited depth of the Si substrate, the epitaxial strain is imposed by constraining laterally the cell to the Si lattice dimensions. Still, the atoms are free to relax in plane by moving to their lowest-energy positions under the influence of the epitaxial strain. Both lattice and atomic relaxations occur vertically. Periodic boundary conditions are imposed in the lateral directions. The total number of atoms is of the order of 200 000. The MC simulations are run at 900 K, within the Metropolis algorithm, yielding fully relaxed structures and average values of stress and energy (chemical potential).

Let us first consider the variation of the total stress and energy in the heteroepitaxial system (which includes the QD, the WL, and the substrate) as a function of the number of steps or, equivalently, the depth of the holes. The size of the problem constrains us to consider a limited number of steps. Nevertheless, the extracted trends with increasing depth are clear, and they are expected to hold for deeper holes as well. Our results are summarized in Fig. 3, which compares the total average stress of the structures with dots located on the terraces between holes to the stress of structures with dots located in the holes along the sequence of steps. There are two remarkable aspects in this variation.

Firstly, we find that the compressive stress in all structures involving a patterned surface is drastically reduced with respect to the nominal stress (QD on the flat surface without patterns). For example, when the pits are just one step deep, stress is reduced by ~13%, corresponding to a drop in energy of ~0.04 eV/atom, which is quite significant in the scale of thermal energies. This result is in good agreement with previous results.[30] Note that the energies of structures having the QD in holes 1 or even 2 ML deep are only slightly higher than the energies of structures having the QD on the terraces. This situation would induce, in the case of shallow holes, a random distribution of dots and polydispersity, in agreement with STM results.[22]

Remarkably, with increasing depth, the near degeneracy between the two cases is lifted and their energies diverge in opposite directions. The stress of structures with dots located on the terraces decreases with increasing the hole depth, while it increases when islands are located in the holes. The trend will be further enhanced if we extrapolate to deeper patterns. In view of this result and noting that the MC method at the ergodic limit approaches the equilibrium state of a system, we readily conclude that it is thermodynamically much more favorable to have preferential nucleation and growth of islands on the terraces rather than in the FIB holes.

It then becomes clear that the various temperature-dependent configurations observed in our experimental work represent distinct phases along the path toward equilibrium. At high T's (750 °C), under conditions of enhanced diffusivity, i.e., when growth is not limited by kinetic barriers, the system reaches the equilibrium state, which dictates ordered arrays of dots on the terraces between the holes. This implies that the material deposited in the holes, whose stepped walls act as nucleation centers, acquires enough energy to overcome the kinetic barriers in order to move out of the pits and assemble on the terraces. Such a result is also observed when Ge is deposited on surface ripples,[26] on mesas,[29] and on nanopatterns[31] in near equilibrium conditions. At low T's (550 °C), on the other hand, there is not enough energy to overcome the diffusion barriers, and Ge is trapped in the holes, giving rise to the metastable ordered phase. A similar situation has been observed in the literature due to the presence of impurities in the pits[32] or due to low surface diffusion of adatoms as reported in Ref. 32. It was found that the final island arrangement depends on the nature of the nanopattern sidewalls,[33] and it was suggested that this may be due to changes in diffusion of Ge across the nonplanar surface.[34] The random mixed phase, with dots both on terraces and in holes, is obviously a saddle point between the metastable and the equilibrium states, resulting from limited out-diffusion of Ge from the pits.

More insight into the stress state of these structures at equilibrium is gained by decomposing the total stress variation into contributions from each component of the system. These are shown in Fig. 4 as a function of depth. We observe two competing factors which shape up the total variation. The destabilizing factor is the increase of the compressive stress in the islands as the depth increases. However, this is drastically counterbalanced by the stabilizing strong reduction of stress in the WL, while stress in the substrate remains

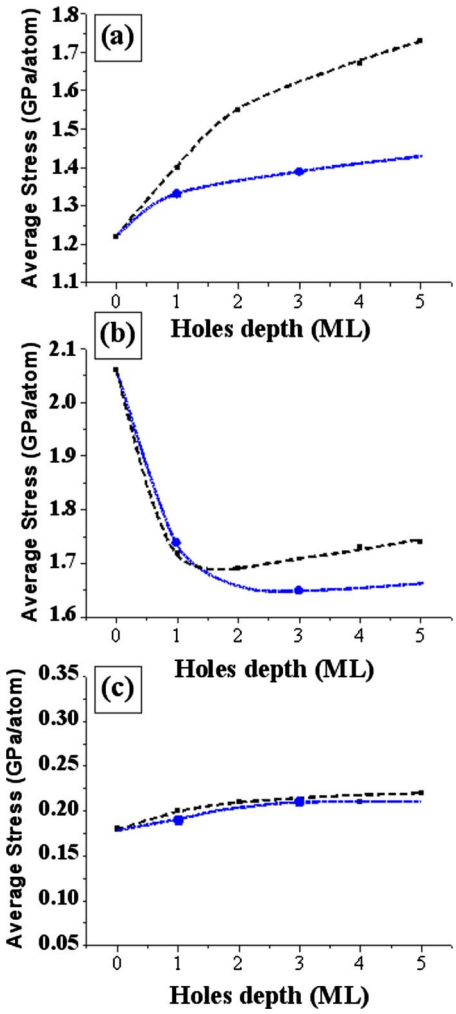

FIG. 4. (Color online) Analysis of stress state in the various components of the QD structure: (a) island, (b) wetting layer, and (c) substrate. Values for structures with islands located on the hole side (terrace) are denoted by dotted lines (solid lines).

more or less constant, giving rise to the overall relief of stress and lowering of energy shown in Fig. 3. Stress in the islands rises more sharply when they grow in the holes. Concurrently, more relief of stress in the WL is achieved when islands grow on the terraces.

These results can be understood as follows. It is well known that steps and the associated domains relax the surface strain energy.[34,35] This allows the drastic relaxation of the compressed WL due to the presence of the stepped pit patterns. Relaxation occurs both at the surface and in subsurface layers. However, when islands grow in the holes, the reduction is less because it is counteracted by the compressive stress induced by the island in the underlayer (WL), mostly in a corral around the periphery.[22] Regarding the increasing stress in the islands, we have two different cases. For islands on the terraces, the slight increase is due to the confining surrounding holes which, as they become deeper, absorb most of the relaxation and thus do not permit sufficient relaxation at the island base, compared to the flat surface. For islands in the holes, the much larger increase is due

to the elongation along the sequence of steps. This produces a rise in stress at the base. Another factor is the increase of the island surface energy as it elongates. An island on the flat terrace has a surface energy per atom equal to −2.9 eV, compared to −2.8 eV when elongated over several step edges. Intermixing which occurs during growth has been investigated using the same modeling as the one described previously.[21] We found that under the present experimental conditions, there is almost no influence of the system configuration (presence or not of patterns) on the mean Ge concentration, neither in the island nor in the wetting layer. Finally, we comment on the significance which the present results might bear on possible applications of highly ordered arrays of QD. Although the metastable phase with islands inside the holes, grown at low T, is superb regarding self-organization processes, it is not convenient for nonvolatile memory applications where insulating oxide needs to be formed below the islands. This is not possible with islands in the holes, but it can be perfectly achieved with islands in the equilibrium phase obtained at higher temperature. Depending on the application desired, it is possible to vary the location of islands.

*Corresponding author. isabelle.berbezier@12mp.fr

[1] S. A. Chaparro, Y. Zhang, and J. Drucker, Appl. Phys. Lett. **76**, 3534 (2000).
[2] G. Hadjisavvas and P. C. Kelires, Phys. Rev. B **72**, 075334 (2005).
[3] O. E. Shklyaev, M. J. Beck, M. Asta, M. J. Miksis, and P. W. Voorhees, Phys. Rev. Lett. **94**, 176102 (2005).
[4] B. Yang, F. Liu, and M. G. Lagally, Phys. Rev. Lett. **92**, 025502 (2004).
[5] Y. H. Tu and J. Tersoff, Phys. Rev. Lett. **93**, 216101 (2004).
[6] P. Raiteri and L. Miglio, Phys. Rev. B **66**, 235408 (2002).
[7] I. Berbezier and A. Ronda, Phys. Rev. B **75**, 195407 (2007).
[8] I. A. Ovid'ko, Phys. Rev. Lett. **88**, 046103 (2002).
[9] B. Ziberi, F. Frost, and B. Rauschenbach, Appl. Phys. Lett. **88**, 173115 (2006).
[10] Z. Zhong, A. Halilovic, M. Mühlberger, F. Schäffler, and G. Bauer, Appl. Phys. Lett. **82**, 445 (2003).
[11] M. De Seta, G. Capellini, and F. Evangelisti, Phys. Rev. B **71**, 115308 (2005).
[12] Z. Zhong, H. Lichtenberger, G. Chen, M. Mühlberger, C. Schelling, J. Myslivecek, A. Halilovic, J. Stangl, G. Bauer, W. Jantsch, and F. Schäffler, Microelectron. Eng. **83**, 1730 (2006).
[13] S. Kiravittaya, M. Benyoucef, R. Zapf-Gottwick, A. Rastelli, and O. G. Schmidt, Appl. Phys. Lett. **89**, 233102 (2006).
[14] C. Dais, H. H. Solak, Y. Ekinci, E. Müller, H. Sigg, and D. Grützmacher, Surf. Sci. **601**, 2787 (2007).
[15] C. J. Moore, C. M. Retford, M. J. Beck, M. Asta, M. J. Miksis, and P. W. Voorhees, Phys. Rev. Lett. **96**, 126101 (2006).
[16] I. Daruka and J. Tersoff, Phys. Rev. Lett. **95**, 076102 (2005).
[17] J. E. Prieto and I. Markov, Phys. Rev. B **72**, 205412 (2005).
[18] A. Karmous, A. Cuenat, A. Ronda, I. Berbezier, S. Atha, and R. Hull, Appl. Phys. Lett. **85**, 6401 (2004); A. G. Nassiopoulou, A. Olzierski, E. Tsoi, I. Berbezier, and A. Karmous, J. Nanosci. Nanotechnol. **7**, 316 (2007).
[19] A. Karmous, I. Berbezier, A. Ronda, R. Hull, and J. Graham, Surf. Sci. **601**, 2769 (2007).
[20] P. D. Szkutnik, A. Sgarlata, S. Nufris, N. Motta, and A. Balzarotti, Phys. Rev. B **69**, 201309(R) (2004).
[21] P. Sonnet and P. C. Kelires, Phys. Rev. B **66**, 205307 (2002); G. Hadjisavvas, P. Sonnet, and P. C. Kelires, *ibid.* **67**, 241302(R) (2003); P. C. Kelires, J. Phys.: Condens. Matter **16**, S1485 (2004).
[22] P. Sonnet and P. C. Kelires, Appl. Phys. Lett. **85**, 203 (2004).
[23] J. Tersoff, Phys. Rev. B **39**, 5566 (1989).
[24] P. C. Kelires and J. C. Tersoff, Phys. Rev. Lett. **63**, 1164 (1989).
[25] In this approach, positive (negative) sign indicates compressive (tensile) stress.
[26] P. D. Szkutnik, A. Sgarlata, A. Balzarotti, N. Motta, A. Ronda, and I. Berbezier, Phys. Rev. B **75**, 033305 (2007).
[27] A. Rastelli and H. von Känel, Surf. Sci. **532-535**, 769 (2003).
[28] P. Raiteri, D. B. Migas, L. Miglio, A. Rastelli, and H. von Känel, Phys. Rev. Lett. **88**, 256103 (2002).
[29] Y. Fujikawa, K. Akiyama, T. Nagao, T. Sakurai, M. G. Lagally, T. Hashimoto, Y. Morikawa, and K. Terakura, Phys. Rev. Lett. **88**, 176101 (2002).
[30] Zhenyang Zhong, W. Schwinger, F. Schäffler, G. Bauer, G. Vastola, F. Montalenti, and L. Miglio, Phys. Rev. Lett. **98**, 176102 (2007).
[31] M. Borgström, V. Zela, and W. Seifert, Nanotechnology **14**, 264 (2003).
[32] A. Portavoce, M. Kammler, R. Hull, M. C. Reuter, and F. M. Ross, Nanotechnology **17**, 4451 (2006).
[33] Z. Y. Zhong, A. Halilovic, T. Fromherz, F. Schaffler, and G. Bauer, Appl. Phys. Lett. **82**, 4779 (2003).
[34] F. M. Ross, M. Kammler, M. E. Walsh, and M. C. Reuter, Microsc. Microanal. **10**, 105 (2004); R. A. Budiman, Phys. Rev. B **72**, 035322 (2005).
[35] O. L. Alerhand, D. Vanderbilt, R. D. Meade, and J. D. Joannopoulos, Phys. Rev. Lett. **61**, 1973 (1988).